CHEMISTRY
A EUROPEAN JOURNAL

DOI: 10.1002/chem.200800342

The Influence of Densely Organized Maltose Shells on the Biological Properties of Poly(propylene imine) Dendrimers: New Effects Dependent on Hydrogen Bonding

Barbara Klajnert,*[a] Dietmar Appelhans,*[b] Hartmut Komber,[b] Nina Morgner,[c] Simona Schwarz,[b] Sven Richter,[b] Bernhard Brutschy,[c] Maksim Ionov,[d] Anatoly K. Tonkikh,[d] Maria Bryszewska,[a] and Brigitte Voit[b]

Abstract: Maltose-modified poly(propylene imine) (PPI) dendrimers were synthesized by reductive amination of unmodified second- to fifth-generation PPI dendrimers in the presence of excess maltose. The dendrimers were characterized by using ^{1}H NMR, ^{13}C NMR, and IR spectroscopies; laser-induced liquid beam ionization/desorption mass spectrometry; dynamic light scattering analyses; and polyelectrolyte titration. Their scaffolds have enhanced molecular rigidity and their outer spheres, at which two maltose units are bonded to the former primary amino groups on the surface, have hydrogen-bond-forming properties. Furthermore, the structural features reveal the presence of a dense shell. Experiments involving encapsulation (1-anilinonaphthalene-8-sulfonic acid) and biological properties (hemolysis and interactions with human serum albumin (HSA) and prion peptide 185-208) were performed to compare the modified with the unmodified dendrimers. These experiments gave the following results: 1) The modified dendrimers entrapped a low-molecular-weight fluorescent dye by means of a dendritic box effect, in contrast to the interfacial uptake characteristic of the unmodified PPI dendrimers. 2) Both low- and high-generation dendrimers containing maltose units showed markedly reduced toxicity. 3) The desirable features of bio-interactions depended on the generation of the dendrimer; they were retained after maltose substitution, but were now mainly governed by nonspecific hydrogen-bonding interactions involving the maltose units. The modified dendrimers interacted with HSA as strongly as the parent compounds and appeared to have potential use as antiprion agents. These improvements will initiate the development of the next platform of glycodendrimers in which apparently contrary properties can be combined, and this will enable, for example, therapeutic products such as more efficient and less toxic anti-amyloid agents to be synthesized.

Keywords: dendrimers · hydrogen bonds · oligosaccharides · peptides · poly(propylene imine) · proteins

[a] Dr. B. Klajnert, Prof. M. Bryszewska
Department of General Biophysics
University of Lodz
12/16 Banacha Street, 90-237 Lodz (Poland)
Fax: (+48) 635-4474
E-mail: aklajn@biol.uni.lodz.pl

[b] Dr. D. Appelhans, Dr. H. Komber, Dr. S. Schwarz, Dr. S. Richter, Prof. B. Voit
Leibniz Institute of Polymer Research Dresden
Hohe Strasse 6, 01069 Dresden (Germany)
Fax: (+49) 351-465-8565
E-mail: applhans@ipfdd.de

[c] N. Morgner, Prof. B. Brutschy
Institute for Theoretical and Physical Chemistry
Johann-Wolfgang-Goethe Universität
Marie-Curie-Strasse 11, 60439 Frankfurt (Germany)

[d] Dr. M. Ionov, Dr. A. K. Tonkikh
Department of Biophysics
National University of Uzbekistan
Vuzgorodok 1, 100174 Tashkent (Uzbekistan)

Supporting information for this article is available on the WWW under http://dx.doi.org/10.1002/chem.200800342. It includes NMR spectroscopic data for unmodified PPI dendrimers **1**–**4** in D_2O; additional figures showing NMR and mass spectra of the modified PPI dendrimers; a table showing the comparison of hydrodynamic radii and surface charge; a table showing the specific charge of unmodified and modified PPI dendrimers; additional spectra for bio-interactions; and data regarding the (surface) composition of HSA.

Introduction

Since the beginning of the 1990s there has been a widely increasing interest in the biological, (bio)medical, and pharmaceutical applications of dendrimers.[1–7] One advantage of this research field is that dendrimers can be synthesized in a controlled manner to form small or large (macro-)molecules with perfectly branched structures, and many of these have valuable and unusual properties.[8] In most cases, the success of dendrimers as precisely constructed and multifunctional working tools arises from their globular shape and the dendritic effect of surface groups. In particular, the properties of dendrimers in these applications depend strongly on the nature of the surface groups that combine, for example, solubility, interaction, and biocompatibility properties.

From the biological, (bio)medical, and pharmaceutical points of view, the surface groups and particularly the surface charge determine the toxicity of a dendrimer.[2a,8] In general, regardless of molecular structure and surface composition, cationic dendrimers are more hemolytic and cytotoxic than neutral and anionic dendrimers.[2a,9] This is because they bind nonspecifically to negatively charged cell membranes resulting predominantly in in vitro and in vivo toxicity. Various studies have indicated that dendritic surface amino groups are the most toxic.[2a,9,10] In contrast, negatively charged and neutral dendrimers, possessing carboxylate or poly(ethylene oxide) (PEO) surface groups, respectively, have proved neither hemolytic nor cytotoxic towards a panel of cell lines in vitro.[10a] The biological properties of neutral dendrimers with poly(ethylene glycol) (PEG) chains attached to the surface can be manipulated positively to prolong their blood circulation time, changing their bio-distribution so that liver accumulation and kidney excretion are decreased.[11] Other modifications of amino surface groups markedly decreased dendrimer toxicity making them suitable as drug and gene delivery systems.[9b,c,12] Also, dendrimers with fatty acid modified surfaces were found to be significantly less cytotoxic than the parent dendrimers and exhibited enhanced permeation through Caco-2 monolayers.[13]

For studies of dendrimers in vitro and in vivo, the greatest challenge for the future is to find the right balance between toxic side effects and biological, (bio-)medical, and pharmaceutical activities (for therapeutic and diagnostic applications). Previous studies have shown that bio-interactions between negatively charged proteins and dendrimers depend on electrostatic forces.[14] Therefore, it has been inferred that cationic dendrimers interact more strongly with negatively charged or acidic proteins than dendrimers with no surface charge. Such electrostatic interactions are crucial for many medical applications, such as the antiviral activities of dendrimers with peptide or anionic surface groups,[15] the biocidic activities of dendrimers with quaternary ammonium groups,[16] and the disruption of amyloid fibrils responsible for neurodegenerative disorders.[17,18] In the last case, the main driving force is the high affinity between cationic dendrimers and protein structures. These observations indicate that amino-terminated poly(amidoamine) (PAMAM) and poly(propylene imine) (PPI) dendrimers have potentially therapeutic activities in prion diseases. In contrast, hydroxyl-terminated PAMAM dendrimers were not active over the same concentration range.[18]

One aim of our work is directed towards developing an improved method for substituting the cationic charges on amino-terminated dendrimers so that they can be used as efficient antiamyloid agents with low cytotoxicity. To obtain the next generation of dendrimers with improved antiamyloid properties, the governing idea was to tune the surface by substituting the cationic charge with hydrogen-bond-forming oligosaccharide units. It should be possible for the oligosaccharide units to suppress the biological processes involved in neurodegenerative disorders by general noncovalent hydrogen-bonding interactions with prion and Alzheimer peptides and proteins. In addition, the attachment of oligosaccharide units to the outer sphere results in remarkably low or zero cytotoxicity towards different cell lines.[10c,19] Our concept was inspired by the following facts: 1) PEGylated dendrimer surfaces are nontoxic and nonimmunogenic and led to the development of unimolecular micelles for encapsulating and releasing drugs.[20] Because the PEG chains are nonionic, these dendrimers have no obvious way of forming the hydrogen-bonding interactions necessary for tailoring biological processes. 2) The field of glycomics[21] has produced a better understanding of the interactions between carbohydrates and various biomolecules and biological systems, in which molecular recognition of (poly-)carbohydrates[22] is the dominant initial step in regulating or suppressing biological processes. Thus, the glycodendrimers are promising for use as multivalent ligands for various bio-interactions,[23,24] for example, for detailed studies of their interactions with multiple cell-surface receptors to develop antiviral agents.[2b,23c] 3) Apart from these investigations of the molecular recognition of biomolecules by the (oligo-)saccharide units of glycodendrimers, no other studies to our knowledge have been devoted to studying nonspecific hydrogen-bonding interactions with proteins and other biological molecules and systems, without molecular recognition of individual (oligo-)saccharide units. 4) Reductive amination is one of the simplest synthetic methods for directly introducing oligosaccharide units without protective groups onto amino-terminated dendrimer surfaces in the aqueous phase.[25] Thus, the starting point of our concept was to synthesize higher-generation PPI dendrimers with densely organized oligosaccharide shells in which each peripheral amino group is modified by two chemically coupled oligosaccharide units (Scheme 1). Such dendrimer structures will provide a platform for developing the next generation of dendrimers, combining apparently contrary properties (e.g., water solubility, nonionic surface groups, neutral charge, nonspecific hydrogen-bond-forming surface groups for modifying biological processes, high biocompatibility, and drug encapsulation–release) more effectively than previously described glycodendrimers.[24] With regard to developing such glycodendrimers, one recent example of a glycodendrimer

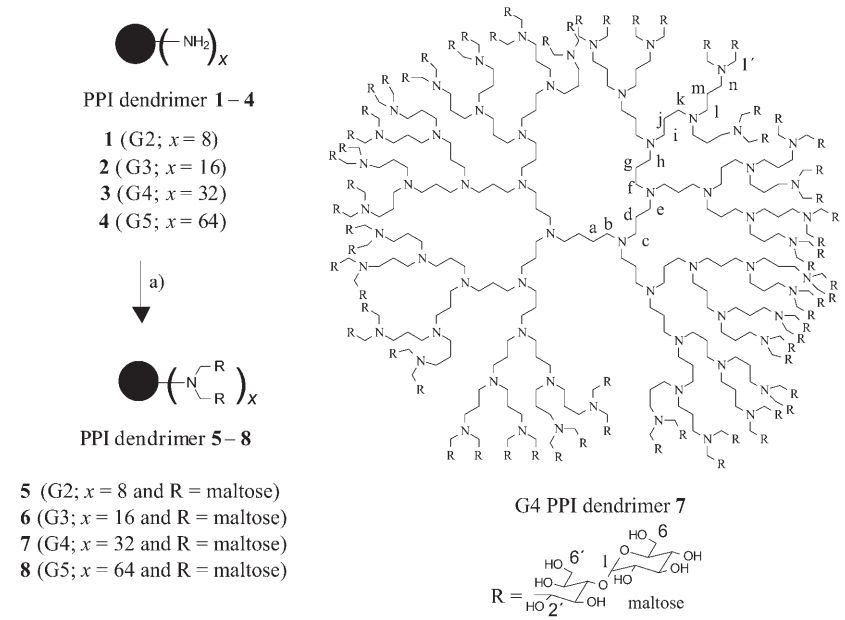

Scheme 1. PPI dendrimers used for the encapsulation of fluorescent ANS and for the bio-interaction investigations with HSA protein and prion peptide $PrP_{185-208}$. a) PPI dendrimers **1–4** with maltose monohydrate (ratio NH_2/maltose (1:20)–(1:24))/BH_3·Py complex in sodium borate solution at 50 °C for 7 d followed by dialysis in distilled water.

that was examined is a mannose-functionalized fifth-generation PPI dendrimer that simultaneously inhibits multiple virus receptors and releases the anti-HIV drug lamivudine.[19b]

In this paper, we report the synthesis and characterization of high-generation PPI dendrimers with maltose shells. This is a first step towards the development of molecular dendritic scaffolds with nonspecific hydrogen-bonding activities for tailoring biological processes. In this context, experiments on biological properties (hemolytic activity, and bio-interactions with prion peptide PrP 185-208 and human serum albumin (HSA) protein) and encapsulation were carried out and the results were compared with those obtained from the unmodified parent PPI dendrimers. The bio-interaction results gave deeper insight into the interactions of both types of dendrimer with HSA under physiological conditions, which led to a new model of protein–dendrimer interactions based on different noncovalent bonds. Furthermore, dendrimers with a crowded maltose shell showed a similar behavior towards PrP 185-208 as positively charged PPI dendrimers.

Results

Synthesis and characterization of maltose-modified PPI dendrimers: To couple two maltose units per surface amino group by using a simple one-pot method, the established technique for reductive amination of monodendrons and dendrimers by various excess oligosaccharides[25,26] was adopted as a synthetic tool for the third-, fourth-, and fifth-generation PPI dendrimers **2–4** in this study. By using this synthetic method, with borane–pyridine complex in sodium borate buffer at 50 °C for 7 d, the desired maltose-modified PPI dendrimers **5–8** were successfully produced after a final dialysis in water for at least 3 d to remove excess maltose (Scheme 1). The results of the reductive amination of dendrimers **1–4** are summarized in Table 1. Dendrimers **5–8** were characterized by using NMR and IR spectroscopies; laser-induced liquid beam ionization/desorption mass spectrometry (LILBID-MS); and dynamic light scattering (DLS) analyses.

The structural characterization of **5–8** is governed by evidence for the complete conversion of the surface amino groups of **1–4**. The proof of the chemical structure of the maltose-modified PPI dendrimers **5–8** was carried out by using ^{13}C NMR spectroscopy. As one example, the ^{13}C NMR spectrum of fourth-generation PPI dendrimer **7** is presented in Figure 1. Generally, the spectra are characterized by broadened signals for the PPI core, whereas the signals of the terminal glucose units are narrow. The signals of the reacted α-glucose unit are broadened and only the main signals could be assigned. By taking into account that carbon atoms 2′ to 5′ of the R group are chiral, one can assume that signals of lower intensity are possibly caused by minor diastereomers of the PPI–$N(CH_2R)_2$ moiety. The absence of signals in the $\delta = 40$–50 ppm region of the ^{13}C NMR spectra also gave evidence that the content of un- or monosubstitut-

Table 1. Reaction conditions and results of the synthesis of maltose-modified PPI dendrimers **5–8** by reductive amination between the precursors (**1–4**) and excess maltose.

Dendrimer	Precursor	No. NH_2 groups of precursor	$-NH_2/-CHO$[a]	Yield [%]	No. coupled maltose units[b]
5	**1** (G2)	8	0.05–0.042	70	15 (16)
6	**2** (G3)	16	0.05–0.042	66	34 (32)
7	**3** (G4)	32	0.05–0.042	91	69 (64)
8	**4** (G5)	64	0.05–0.042	98	130 (128)

[a] Molar ratio between the terminal amino groups of the precursor and the reducing unit of maltose. [b] Determined by using ^1H NMR spectroscopy using the integral ratio of the anomeric CH-group signal of maltose to that of the internal $-CH_2\mathbf{CH_2}CH_2$ groups of the dendritic PPI matrix taking into account the PPI generation (estimated error: ±2%); the number in brackets presents the theoretical value for 100% conversion of amino functionalities.

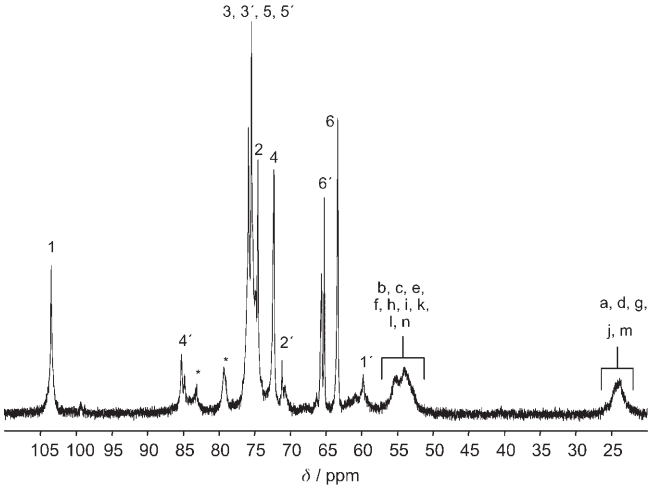

Figure 1. ^{13}C NMR spectrum of **7** in D_2O with signal assignment. The atom positions correspond with those shown in Scheme 1. The asterisks (*) indicate unassigned maltose signals.

ed terminal amino groups of the PPIs should be very low. A previously described determination was applied to calculate the degree of PPI substitution by using ^1H NMR spectroscopy.[25] The intensity of the anomeric CH-group signal of the maltose ($\delta = 4.95$–5.35 ppm) was related to the signal intensity of the internal CH_2 groups of the dendritic PPI matrix ($\delta = 1.4$–2.3 ppm) while taking into account the different generations. Within the limits of this method it was found that 95% (for **5**) up to about 100% (for **6**–**8**) of the NH functionalities were converted with maltose (Table 1). More detailed structural characterization of the chemically coupled maltose units on the dendrimer surfaces was achieved by using LILBID-MS analyses. The mass spectrum of **8** is presented in Figure 2. The mass spectrometry results (Table 2) showed the desired degree of substitution by maltose on the surfaces of PPI dendrimers **5**–**7**, but not **8**. Finally, DLS measurements showed the expected increase in hydrodynamic radius (R_h up to 3.5 nm) with increasing generation number of the maltose-modified PPI dendrimers **5**–**8** (Table 1-SI in the Supporting Information). Under the conditions used, there was no indication of aggregated PPI macromolecules in the aqueous phase.

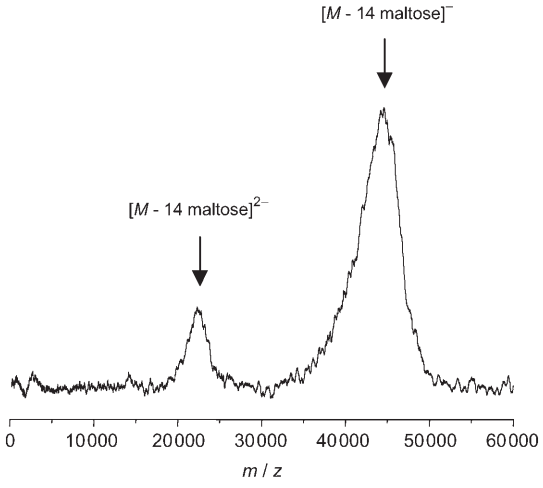

Figure 2. LILBID-MS spectrum of **8** (49062.9 g mol^{-1}).

Table 2. Determination of the molecular weight (M_r) of PPI dendrimer **5**–**8** by LILBID-MS analyses and the number of chemically attached maltose units (MU); comparison between theoretical (theor) and observed (obsd) data.

Dendrimer	M_r [g mol^{-1}]		Number of MU	
	theor[a]	obsd	theor	obsd[b]
5[c]	5994.0	≈6000	16	16
6	12128.3	≈12100	32	32
7	24396.8	≈24400	64	64
8	49062.9	≈44500	128	≈114

[a] M_r based on the empirical formula with 100% converted primary amino groups. [b] Number of MU calculated from the observed molecular weight. [c] Described in ref. [24c].

Hemolysis test: Red blood cell lysis is a simple, widely used method for studying membrane alterations. The hemoglobin release can be quantified. For the unmodified PPI dendrimers **1** and **3**, hemolysis was both concentration- and generation-dependent (Figure 3). Two-hour incubations with the unmodified second- and fourth-generation PPI dendrimers at concentrations of 3 and 6 mg mL^{-1} proved to be very destructive for erythrocytes. The counterparts of these dendrimers (both generations) with attached maltose units showed almost complete loss of hemolytic activity.

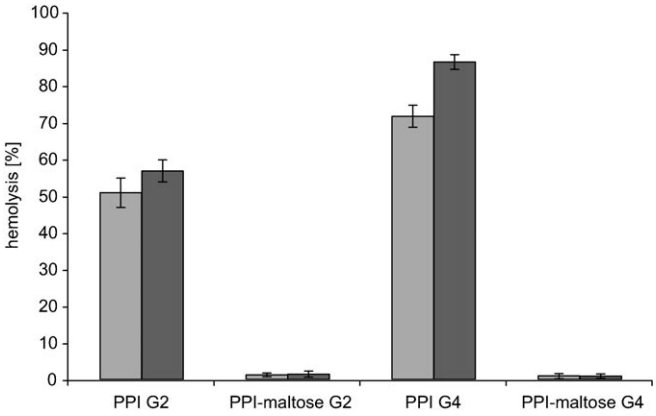

Figure 3. Hemolysis induced by incubation of red blood cells with dendrimers **1** (PPI G2), **3** (PPI G4), **5** (PPI–maltose G2), and **7** (PPI–maltose G4) at concentrations of 3 (pale gray) and 6 mg mL^{-1} (dark gray).

Interaction with human serum albumin (HSA): The basic information obtained from fluorescence measurements relates to the molecular environment of the chromophore. The fluorescence of tryptophan (Trp) residues is very sensitive to changes in their vicinity, so it is widely used to study changes in the molecular conformations of proteins. HSA possesses

one tryptophan residue located at the bottom of the hydrophobic pocket in subdomain IIA (Trp-212). Therefore, protein–dendrimer interactions can be evaluated by studying changes in the fluorescence spectra. The strength of the interaction was calculated by using the Stern–Volmer equation, through analysis of the decrease in fluorescence intensity of the Trp residue in HSA. As one example, the fluorescence spectra of HSA in the presence of increasing amounts of maltose-modified fourth-generation **7** are presented in Figure 4. No changes were noted in the position of the signals of the emission spectrum or in the shape of spectrum.

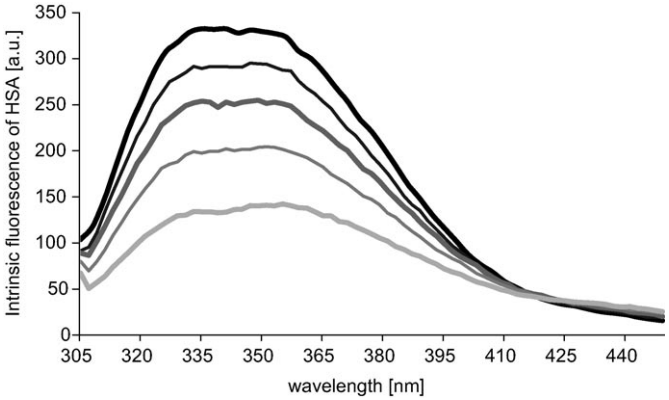

Figure 4. Changes in the HSA spectrum upon addition of the fourth-generation dendrimer **7**. Dendrimer concentrations starting from the top: 0, 0.073, 0.188, 0.333, and 0.600 mmol L^{-1}. $\lambda_{exc} = 295$ nm.

The quenching effect was analyzed according to the following Stern–Volmer equation [Eq. (1)]:[27]

$$\frac{F_0}{F} = 1 + K_{SV}[Q] \quad (1)$$

in which F_0 and F are the fluorescence intensities in the absence and presence of quencher, respectively, K_{SV} is the Stern–Volmer dynamic quenching constant, and [Q] is the concentration of the quencher. The Stern–Volmer constants express the accessibility of the chromophore to the quencher. The equation assumes a linear plot of F_0/F versus [Q] and the slope is K_{SV}. K_{SV} values for the maltose-modified PPI dendrimers **5**–**8** were calculated from the plots shown in Figure 5 and are presented in the graphs. K_{SV} values for the unmodified PPI dendrimers are presented in the Supporting Information (Figure 6-SI). The following results were obtained concurrently: 1) The strengths of the interaction for the unmodified second-generation PPI dendrimer **1** and the maltose-modified second- and third-generation PPI dendrimers **5** and **6** were similar and very low, which indicates no interaction. 2) The third-generation **2** interacts about three times more strongly than its maltose-modified counterpart **6**, which indicates a weak interaction with HSA. 3) The unmodified and maltose-modified fourth- and fifth-generation **3**, **4**, **7**, and **8** showed similarly strong interactions with HSA; the unmodified fifth-generation **4** interacted most

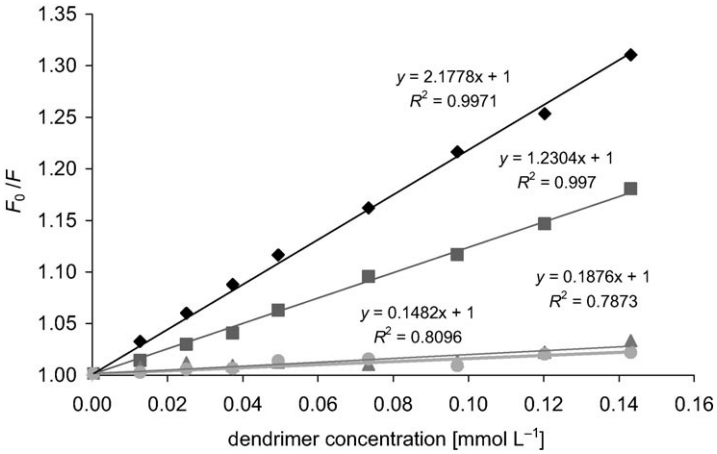

Figure 5. Stern–Volmer plots for tryptophan fluorescence quenching by maltose-modified dendrimers **5** (●), **6** (▲), **7** (■), and **8** (◆).

strongly. Larger constants were obtained for the unmodified dendrimers, although changes in interactions with the protein after surface modification were not very significant.

Effects of dendrimers on aggregation of the prion peptide: Because ThT fluorescence is sensitive to the presence of amyloid fibrils it can serve as a good indicator of fibril formation. In our experiments, amyloid fibrils were formed in vitro and the process was monitored over time. Figure 6 shows the variation in ThT fluorescence in the presence of PrP 185-208 (structure of PrP 185-208 shown in Figure 7) in the absence and presence of the maltose-modified PPI dendrimers **5**–**7** (Figure 6). Sigmoid curves typical of a nucleated polymerization reaction were observed. Analyzing the shape of the curve enables two important parameters to be compared: the reaction rates (the nucleation rate given by the extension of the lag phase, and the elongation rate given by the exponential part of the sigmoid), and the final concentration of amyloid fibrils (the level of fluorescence reached at the plateau). During the lag phase, peptide monomers slowly combine to form nonfibrillar structures known as nuclei. Addition of peptide monomers to these nuclei and interactions among the nuclei, together with a conformational transition that implies the formation of fibrillar β-sheet structures, results in the so-called elongation phase (the faster, exponential part of the sigmoid). From the graphs, the duration of the nucleation phase can be estimated by determining the point at which the extrapolated exponential part of the sigmoid cuts the time axis, and the elongation rate is measured as the slope of the exponential part (Figure 7-SI).[17b] Dendrimer **7** at concentrations of 5.5 and 10 μmol L^{-1} and dendrimer **6** at a concentration of 10 μmol L^{-1} completely inhibited fibril formation in the time interval monitored (Figure 6). The effect was generation-dependent, and for the highest tested generation (fourth) even the concentration of 5.5 μmol L^{-1} caused complete inhibition. Lower concentrations of all dendrimers (1 μmol L^{-1}) accelerated both the nucleation and elongation phases, and

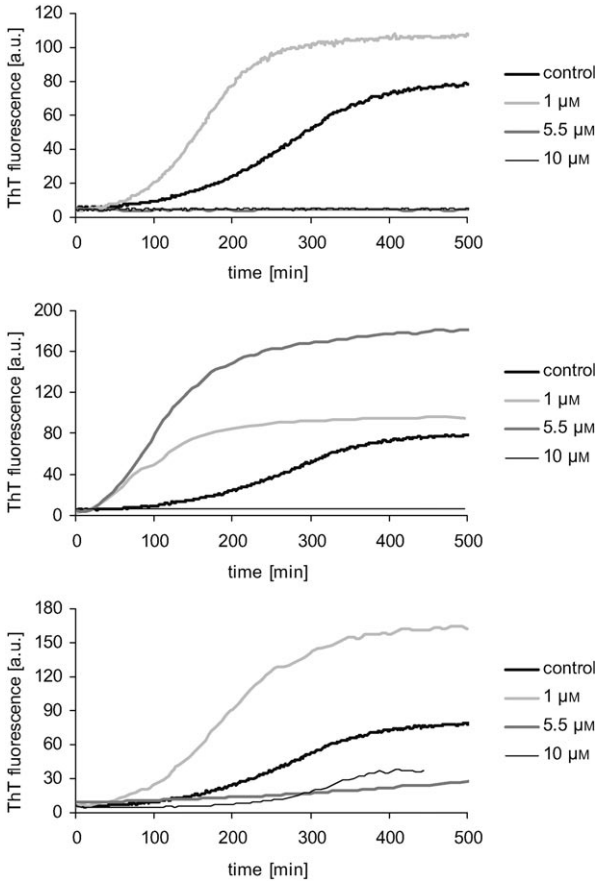

Figure 6. Changes in the fluorescence of ThT during the aggregation process of PrP 185-208 peptide in the presence of the maltose-modified dendrimers **7** (top), **6** (middle), and **5** (bottom)

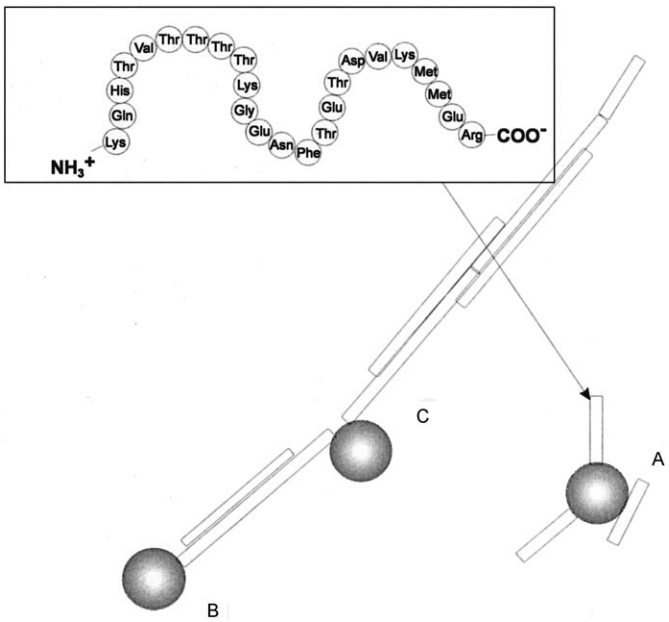

Figure 7. Three main mechanisms of possible antiamyloid activity of dendrimers: A) interactions with peptide monomers, B) blocking fibril ends, C) breaking of fibrils. Chemical structure of the PrP 185-208 peptide is shown in the frame and the gray spheres are the dendrimer.

the final amount of fibril created was greater than that in the control.

Interactions with 1-anilinonaphthalene-8-sulfonic acid (ANS): The encapsulation properties of dendrimers can be assessed by studying the fluorescence of small molecules in their presence. The fluorescent dye, ANS, used in this study has a low fluorescence yield in polar environments, but this is greatly enhanced as the solvent polarity decreases. This enhancement is accompanied by a blueshift of the emission wavelength. Both these phenomena were observed upon addition of dendrimers. ANS had an approximately twofold higher fluorescence intensity in the presence of the maltose-modified dendrimers (Figure 8). Moreover, these dendrimers caused a greater blueshift (Figure 9 and the Supporting Information). The unmodified and modified second- and third-generation dendrimers only changed the fluorescence properties of ANS slightly, if at all. The binding constant (K_b) and the number of binding centers per dendrimer molecule (n) for the fourth and fifth generations were deter-

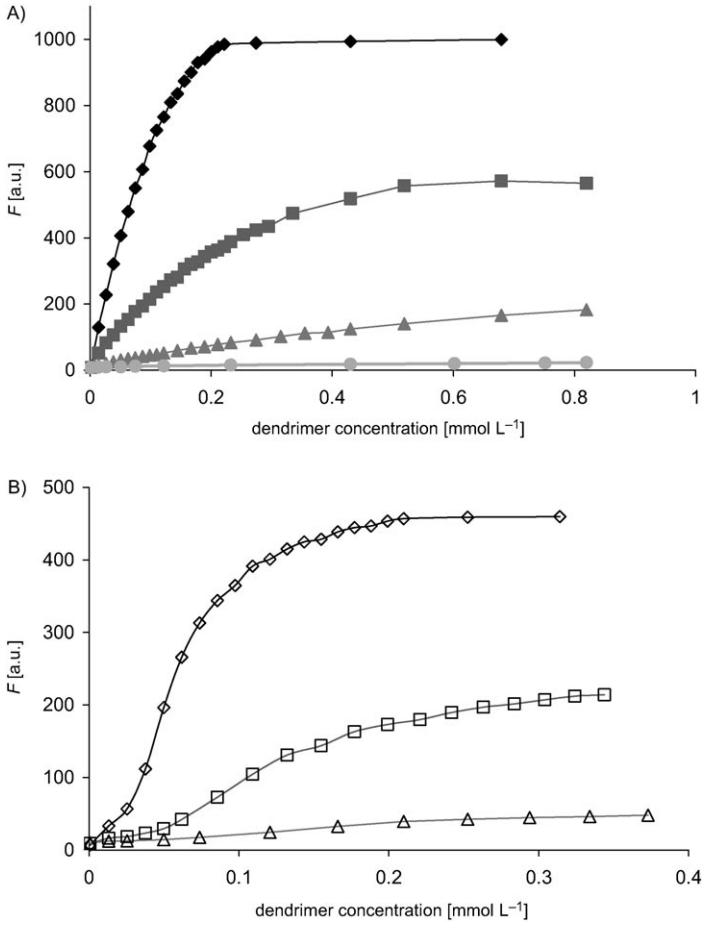

Figure 8. Changes in the ANS fluorescence intensity recorded at $\lambda =$ 470 nm upon addition of A) maltose-modified (● = G2; ▲ = G3; ■ = G4; ◆ = G5) and B) unmodified (△ = G3; □ = G4; ◇ = G5) PPI dendrimers using $C_{ANS} = 20\ \mu mol\ L^{-1}$.

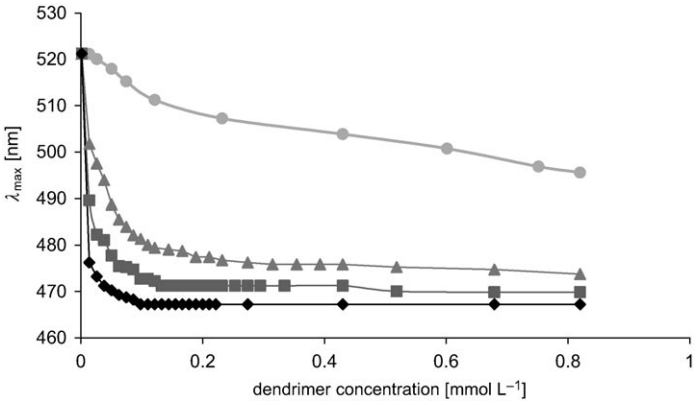

Figure 9. Changes in the position of the emission maximum of ANS upon addition of maltose-modified PPI dendrimers (●=G2; ▲=G3; ■=G4; ◆=G5) using $C_{ANS}=20\ \mu mol\,L^{-1}$.

mined by a double fluorometric titration approach by using the Scatchard method. Graphs of $C_{dendrimer}/C_{ANS}^{bound}$ on the ordinate versus $1/C_{ANS}^{free}$ on the abscissa were drawn and linear regression gave the values of K_b and n. These values are summarized in Table 3. For both maltose-modified and unmodified dendrimers, the number of binding centers increased with increasing generation number and was always a little higher for maltose-modified dendrimers. Interestingly, the binding constants were greater for the unmodified PPI dendrimers.

Table 3. Binding constant (K_b) of ANS and the number of binding centers per molecule of dendrimer (n).

	Unmodified dendrimer		Modified dendrimer	
	G4	G5	G4	G5
n	0.12	0.41	0.16	0.53
K_b [l mol^{-1}]	1.11×10^5	5.11×10^5	2.82×10^4	2.52×10^4

Discussion

Reductive amination, used as a synthetic tool in this study, modified the amino-terminated PPI dendrimer surfaces as desired, mainly leading to two bound maltose units per peripheral amino group. The mass spectrometry results (Table 2 and Figure 2; Figures 3-SI and 4-SI in the Supporting Information) indicate a high degree of maltose substitution on the PPI dendrimer surface; only the fifth generation showed on average a lower degree of maltose substitution than predicted theoretically. Thus, it can be claimed that multiple application of reductive amination is a highly efficient method for converting the PPI dendrimer surface. In particular, the surface secondary amino groups, formed intermediately by substitution with single maltose units, are accessible and readily undergo a second maltose substitution.

To explain the biological properties of the maltose-modified dendrimers **5**–**8**, mentioned below, it is necessary first to discuss the molecular shape and surface charge of both the unmodified and maltose-modified types. In a previous publication we proposed that **5** is a "dense-shell dendrimer", in contrast to the unmodified PPI dendrimer **1**, which has an open ellipsoidal structure.[25c] This assumption is based on the fact that two chemically coupled maltose units are bulky compared with a surface primary amino surface group, so a crowded oligosaccharide shell is formed on the dendrimer surface. This assumption was supported by molecular modeling.[25c] Such dense-shell dendrimers are only available at higher generations (fourth and fifth) for the unmodified and amino-terminated PPI dendrimers **3** and **4**, which have globular shapes and include potential cavities. Thus, all the maltose-modified dendrimers **5**–**8** can be considered spherical-like dense-shell dendrimers possessing a crowded maltose shell and larger hydrodynamic radii (Table 1-SI in the Supporting Information). This also implies a lower flexibility of the dendritic PPI scaffold and a higher probability of defined cavities within the scaffold relative to the unmodified PPI dendrimers **1**–**4**. In addition, the outer functional groups and molecular subunits of the unmodified PPI dendrimers show some back-folding properties, which can be excluded for **5**–**8**. Further, zeta-potential measurements and polyelectrolyte titration experiments (Table 2-SI in the Supporting Information) confirmed that the unmodified PPI dendrimers **1**–**4** have more highly positively charged surfaces than the nearly neutral maltose-modified PPI dendrimers **5**–**8** in the buffer solutions used for biological and encapsulation studies. Because the strength of a positive charge decreases exponentially with increasing distance, the outer neutral maltose shell precludes the presence of higher positive charges on **5**–**8**. Generally, two types of dendrimers are used for our biological studies: 1) the cationic PPI dendrimers **1**–**4** with open and globular molecular shapes, flexible dendritic scaffolds, and back-folding properties of their outer functional groups and molecular subunits; and 2) the nearly neutral maltose-modified dendrimers **5**–**8** with densely organized maltose units that interact preferentially by hydrogen bonding.

When any type of dendrimer is assessed or discussed as promising for biomedical applications, its toxicity should be evaluated. A hemolysis test is one of the quickest and most informative methods. The data obtained in such an assay give a qualitative indication of the damage that dendrimers can potentially cause when administered intravenously. In our work we compared the hemolysis initiated by unmodified and maltose-modified PPI dendrimers. It is well known that amino-terminated dendrimers cause hemolysis because of interactions between their charged groups and the red blood cell membranes. Two generations were tested: **1** and **5** for the second generation and **3** and **7** for the fourth generation. The attachment of maltose units to the surface decreased the hemotoxicity for both generations. In other words, for both generations, the densely organized maltose units created a shell on the PPI dendrimer surface that sepa-

rated the erythrocytes from the potentially toxic PPI cores of dendrimers **5** and **7** (Figure 3). The results obtained are in agreement with previous studies in which coating of fifth-generation PPI dendrimers with mannose or galactose reduced hemotoxicity.[19a,28] In these cases the peripheral amino groups were substituted by only single monosaccharide units in the outer shell.

After obtaining this evidence that maltose-modified PPI dendrimers are nonhemotoxic, further biological experiments focused on the interactions of dendrimers with maltose shells with proteins, peptides, and other molecules. A specific aim was to retain the desirable properties established for the previously described dendrimers. One such desirable property is the ability of dendrimers **5**–**8** with densely organized maltose units in the outer shell to interact with proteins. Such novel dendrimer architecture can lead to the development of new diagnostic and therapeutic agents such as antibacterial or antiprion agents.

In our previous experiments,[14a–c] the properties and strengths of interaction of hydroxy-, carboxy-, and amino-terminated PAMAM dendrimers with bovine and human serum albumin were tested. The fourth-generation PAMAM dendrimers showed a particularly impressive strong interaction with bovine serum albumin. These dendrimers clearly demonstrated an ability to quench intrinsic protein fluorescence. The interactions involved were driven by electrostatic forces and were strongest for the cationic amino-terminated dendrimers. Thus, a working model was proposed for the interaction between the dendrimers and the protein: the spherical fourth-generation dendrimers created a layer on the protein surface. Before starting our bio-interaction experiments with HSA we assumed that electrostatic interactions dominate the binding of unmodified PPI dendrimers to the anionic charge of HSA. In contrast, we presumed that the PPI dendrimers with maltose shells would interact less strongly with HSA because their surface groups are nonionic and form hydrogen bonds. Surprisingly, in the present comparative study, the unmodified and maltose-modified PPI dendrimers interacted similarly with HSA. Further conclusions from this bio-interaction study were that the interactions were generation-dependent; on average, the unmodified PPI dendrimers (except **3**) interacted slightly more strongly with HSA. It can clearly be seen that the hydrogen-bond-forming maltose shell can interact just as strongly through noncovalent interactions as the cationic surface of the unmodified PPI dendrimers. It should be noted that the sizes and molecular weights of the two types of dendrimer are completely different (Table 1-SI in the Supporting Information).

In view of all the evidence obtained about the bio-interactions of low- and high-generation dendrimers with HSA, we propose the following details of the suggested working model for "dendrimer interaction with a negatively charged protein", presented in Figure 10, which differs from our previously suggested working model of "dendrimer-layered interaction with negatively charged protein":[14a] 1) Irrespective of the surface charge on the dendrimer, the bio-interaction is generation-dependent, starting from the fourth generation. 2) The (surface) composition of HSA shows that, besides the well-known electrostatic interaction between a cationic dendrimer and the anionic protein surface, hydrogen bonds are also formed with the carboxylate groups and oxygen atoms of the amide groups of the proteins (see the Supporting Information). 3) A possible common mechanism for the bio-interaction requires the dendrimer to have an appropriate size and molecular shape; the fourth and higher generations have the necessary spherical shape and rigid molecular architecture. Therefore, the interplay of size and molecular rigidity and the capacity of the dendrimer surface to undergo noncovalent interactions are the main prerequisites for interaction with a sufficiently large area of the negatively charged protein surface at pH 7.4. Once the initial contact surface is formed between dendrimer and protein, further surface contacts can readily be formed, which result in greater rearrangements of i) the tertiary structure of HSA and ii) the surface of HSA, as indicated by the fluorescence quenching of the internal Trp residue. 4) Because of the differences in size and molecular weight between the two types, the cationic PPI dendrimers tend to form more contacts with HSA than the maltose-modified dendrimers **7** and **8** (Figure 10). We cannot currently propose further details of the interactions between **7** and **8** and HSA beyond the very simplified model in Figure 10; these interactions are under further investigation.

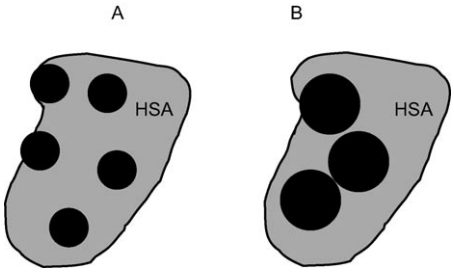

Figure 10. Models of the interactions between unmodified PPI dendrimers (A) or maltose-modified PPI dendrimers (B) with HSA for the fourth and fifth generation. Unmodified PPI dendrimers (A) are present in higher numbers enabling them to make more contact points on the surface of the HSA molecule than the maltose-modified dendrimers. For case "A" there is no complete covering of the unmodified PPI dendrimer on the HSA surface.

Encouraged by these results, we decided to investigate whether maltose-modified dendrimers affect the creation of fibrils, which is a hallmark of prionoses and generally of all amyloidoses. Instead of working with prion-infected cells or brain homogenates we used a previously studied model, prion peptide PrP 185-208 (Figure 7).[29] When this peptide is subjected to low pH and addition of heparin, it creates long fibrils. In a previous study, cationic PPI dendrimers were shown to affect this process.[30] In particular, the third-generation PPI dendrimers at a concentration of 4 $\mu mol\,L^{-1}$ completely inhibited fibril formation, whereas the lowest concentration tested, 1 $\mu mol\,L^{-1}$, sped up the process. A very similar pattern was observed for the fourth-generation

maltose-modified PPI dendrimers (Figure 6). Under the same experimental conditions, 10 μmol L^{-1} concentrations completely inhibited the formation of fibrils from PrP 185-208, and ten times lower concentrations accelerated the process. There are three possible modes of action of antiprion agents, as presented in Figure 7: A) The agent can lower the effective concentrations of peptides that are capable of growing into fibrils by binding to the peptide monomers. B) Amyloid formation can be inhibited by blocking the fibril ends. C) The agent can break the fibrils. A moderate level of fibril breakage in amyloidogenic processes may be responsible for speeding up the formation of aggregates by creating new free ends that can expand when new peptides are attached. However, if breakage is very fast, it can progressively break down all the fibrils until only monomers are left. Therefore, if fibril breakage is the predominant mechanism of inhibition, inhibitors administered in low doses can in fact accelerate fibrilogenesis by providing more ends that serve as replication sites. In higher doses, however, these inhibitors can be effective. This pattern was previously observed for cationic PAMAM and PPI dendrimers. Therefore, which pattern is more useful remains a topic of controversy in the search for new therapeutic agents. From one point of view, it is desirable to preclude fibril formation (which was observed for the higher dendrimer concentration). On the other hand, it has been proposed that short fragments, the so-called protofibrils, are the most toxic species and are probably responsible for brain damage.[17a] If that is the case, then, paradoxically, speeding up the process of fibril formation may be considered desirable. Such behavior was observed when low dendrimer concentrations were used. No matter which pattern is explored further, it should be stressed that the main novelty of the results obtained in this study is related to the type of dendrimer. To date, the literature has reported that amino-terminated dendrimers are effective antiamyloid agents. The main drawback of these cationic dendrimers is their high toxicity. Modification of the dendrimer surfaces with maltose significantly reduces the toxicity, as indicated by their very low hemotoxicity (Figure 3). PPI dendrimers **6** and **7** show that maltose-modified dendrimers can be as potent as amino-terminated dendrimers, though somewhat higher concentrations have to be used.

These two examples of bio-interaction, with HSA and the prion peptide 185-208, clearly show that the surface-modified PPI dendrimers retain the desirable features of the unmodified dendrimers. Bio-interactions involving PPI dendrimers with densely organized maltose shells are governed more by their hydrogen-bonding hydroxyl groups, opening the possibility of using such dendrimers as a platform for developing the next generation of multifunctional dendritic macromolecules as therapeutic and diagnostic agents. Dendrimers with chemically coupled oligosaccharide units have the desirable property of undergoing various bio-interactions by means of their outer shells. The unification of simultaneous encapsulation–release properties with the modification of biological processes by the outer oligosaccharide shell will be the next level of multifunctional diversity of such dendrimers. In the literature, glycodendrimers are also described as promising carrier molecules for drug delivery. Sugar–dendrimer conjugations are considered exciting drug-delivery systems because of the high specificity of carbohydrate–protein interactions that are integral to receptor-mediated endocytosis.[19a] Also, lectin receptors have been found on the surfaces of macrophages, the cells targeted by HIV. Lectin receptors act as molecular targets for sugar molecules. That is why mannosylated PPI dendrimers encapsulating the anti-HIV drug lamivudine provided better targeting and greater activity than the free drug.[19b] In all these cases only one mono- or oligosaccharide unit was introduced per surface functional group, in contrast to the dendrimer architectures with maltose units used in this study.

To evaluate the improved encapsulation properties of PPI dendrimers with densely organized maltose shells relative to the unmodified dendrimers, ANS was used as a model dye; it has a sulfonate group. As expected, the binding constants for the maltose-modified dendrimers were an order of magnitude less than those for the unmodified PPI dendrimers. This is attributable to the diminished cationic charge on the dendrimer surface when the primary amino groups are substituted with maltose units. ANS is negatively charged so the amino groups of the unmodified PPI dendrimers **3** and **4** interact with its sulfonate group. However, the number of binding centers in the maltose-modified dendrimers **7** and **8** was greater, probably because the dendritic structure was more extended. Not only did this structure provide more space, it also allowed for much deeper incorporation, placing the ANS in a more hydrophobic microenvironment, which resulted in a bigger fluorescence blueshift. In the presence of the maltose-modified dendrimers, the maximum of the spectrum shifted to 466 nm for the fifth generation, 470 nm for the fourth generation and 474 nm for the third generation (Figure 9). For unmodified dendrimers these values were 477, 482, and 493 nm, respectively, but the fluorescence intensity was lower (see the Supporting Information). ANS is a fluorescent probe often used to study protein properties, and its location in, for example, HSA is well recognized: it is believed to be located in a hydrophobic pocket. The emission maximum of ANS within HSA is at 466 nm.[31] It can be concluded that the microenvironment of ANS within the maltose-modified dendrimers is similar to its microenvironment in HSA. Therefore, we can conclude that the maltose-modified dendrimers act as dendritic boxes and the encapsulation of ANS is mainly driven by hydrophobic forces, as indicated by the lower binding constants (Table 3). It is probable that the bulky maltose surface effectively screens the internalized ANS from solvent molecules. The encapsulation of ANS by monosaccharide-modified seventh- and eighth-generation PAMAM dendrimers showed similar behavior, but with less blueshifting of the ANS fluorescence.[32] In unmodified PPIs electrostatic interactions held the ANS closer to the surface and led to shallower incorporation. In brief, interfacial uptake of ANS occurs in the unmodified cationic PPI dendrimers. This is consistent

with previous studies in which the antituberculosis drug rifampicin was loaded within mannosylated PPI dendrimers.[19a] As proposed here for ANS encapsulation, hydrophobic interactions and hydrogen bonding contributed to the physical binding of the drug molecule inside the dendritic structure.

Conclusion

In summary, reductive amination is a highly efficient tool for synthesizing PPI dendrimers with densely organized maltose shells based on the introduction of two maltose units per peripheral amino group. Thus, increasingly spherical dense-shell dendrimers up to the fifth generation were produced. Their biological effects on hemolysis and bio-interactions with HSA and the prion peptide PrP 185-208 were then explored and compared with those of the unmodified PPI dendrimers.

To summarize, the dense-shell PPI dendrimers showed several beneficial properties. 1) The coupled maltose units markedly reduced the toxicities of both low- and high-generation PPI dendrimers relative to the unmodified types. 2) The modified dendrimers act as dendritic boxes encapsulating ANS, in contrast to the interfacial uptake of this dye by the unmodified PPI dendrimers. 3) The dendrimers retain the desirable features of bio-interactions, mainly governed by the hydrogen-bond-active maltose units. Surprisingly, this results in a similar strength of interaction with HSA and their potential use as antiprion agents. Therefore, the present study has clearly shown that the nonspecific hydrogen-bonding interactions by PPI dendrimers with crowded maltose shells can do the same work as electrostatic bonding by positively charged PPI dendrimers. This offers a new perspective in the use of dendrimers with densely organized oligosaccharide shells for therapeutic and diagnostic applications. Furthermore, the bio-interaction with HSA, proposed as an enlarged working model for the interactions of (un-)charged dendrimers with proteins, is mainly governed by the formation of contacts with the protein surface caused by a generation-dependent combination of the molecular rigidity of the dendrimer and noncovalent interactions such as electrostatic and nonspecific hydrogen bonds.

Finally, the biological and encapsulation studies showed us that only the fourth- and fifth-generation maltose-modified PPI dendrimers are suited for developing the next generation of more-targeted dendritic macromolecules with various properties (e.g., combining encapsulation–release with modification of a biological process) as therapeutic and diagnostic agents. Thus, the desirable features of nontoxic antiamyloid agents with no cationic charges can be attained, as shown in this study, to initiate the next development of more efficient antiamyloid agents.

Experimental Section

Materials: The second- (DAB-Am8, **1**), third- (DAB-Am16, **2**), fourth- (DAB-Am32, **3**), and fifth-generation (DAB-Am62, **4**) PPI dendrimers were supplied by SyMO-Chem (Eindhoven, The Netherlands). D-(+)-Maltose monohydrate, sodium borate, and the borane–pyridine complex (BH_3·Py, 8 M solution in THF) were used as purchased from Fluka.

The synthetic prion peptide PrP 185-208 [KQHTVTTTTKGENFTETDVKMMER] was purchased from JPT Peptide Technologies GmbH (Germany). ANS and essentially fatty acid free (fraction V) HSA were purchased from Sigma (Germany). HSA was used without further purification. All other chemicals were of analytical grade. For the biological experiments double-distilled water was used.

Characterization of dendrimers: The NMR spectroscopy measurements were carried out on a Bruker DRX 500 NMR spectrometer operating at 500.13 MHz for ^{1}H and at 125.75 MHz for ^{13}C using D_2O as solvent. Sodium 3-(trimethylsilyl)-3,3,2,2-tetradeuteropropionate was added for internal calibration ($\delta(^{13}C)=0$ ppm; $\delta(^1H)=0$ ppm). The signals were assigned by using a combination of 1D and 2D NMR experiments using the standard pulse sequences provided by Bruker. The signal assignments for **6** and **8** can be found in the Supporting Information. The IR spectroscopic investigations were carried out on a Bruker IFS66 spectrometer equipped with a Golden Gate Diamond ATR-Unit (SPECAC) equipped with heating capability. 100 scans for one spectrum were added at a spectral resolution of 4 cm^{-1}. LILBID-MS analyses were used to determine the molar mass of **6–8**; the method is described elsewhere.[33] The dendrimer samples were prepared in aqueous solution with concentrations of 5×10^{-5} for **6** and **7** and 1×10^{-5} M for **8**. All measurements were performed in anionic or cationic mode. DLS experiments were performed at a scattering angle of $\theta=90°$ using an ALV goniometer system (model: ALV/CGS-8FS/N 025). Further details of the system, the concentration used, and calculation of hydrodynamic radii are described elsewhere.[25c] Charge densities (q) of unmodified and modified PPI dendrimers were determined by polyelectrolyte titration in a particle charge detector (PCD-03, Mütek, Germany) combined with a 702 SM Titrino instrument (Metrohm, Switzerland). Solutions of low-molecular-weight sodium polyethylene sulfonate (PES–Na) or poly(diallyldimethylammonium chloride) (PDADMAC) were used as titrants for cationic and anionic systems, respectively. q [meq g^{-1}] was calculated according to Equation (2):

$$q=\frac{C_{\text{titrant}}V_{\text{titrant}}}{Vm} \tag{2}$$

in which C_{titrant} is the concentration of titrant [meq L^{-1}], V the volume of titrated solution, V_{titrant} the equivalent titrant volume, and m is the content of polyelectrolyte in the titrated solution [g L^{-1}].

Synthesis of maltose-modified PPI dendrimers: Maltose-modified second-generation PPI **5** was synthesized according to the literature.[24c]

Maltose-modified third-generation PPI ***6***: Third-generation PPI dendrimer **2** (0.2 g, 1.186×10^{-4} mol), D-(+)-maltose monohydrate (14.74 g, 40.9 mmol), and the borane–pyridine complex (5 mL, 40 mmol, 8 M solution) were dissolved in a sodium borate buffer (37.5 mL, 0.1 M) solution. The reaction solution was stirred at 50 °C for 7 d. The crude product was then purified by dialysis towards deionized water for 3 d. Dendrimer **6** was obtained (0.95 g, 66 %) from 1) distillation of water under reduced pressure followed by drying under vacuum or 2) freeze-drying. ^{1}H NMR (D_2O): $\delta=1.4$–2.3, 2.3–3.4, 3.4–4.55, 4.95–5.35 ppm (see Figure 1A-SI in the Supporting Information); ^{13}C NMR (D_2O): $\delta=22$–24.5, 25.1, 52–56, 59.7, 63.3, 65.2 and 65.6, 71.0, 72.3 and 72.4, 74.5, 75.4 and 75.5, 75.8, 84.8 and 85.2, 103.5 ppm (Figure 1B-SI in the Supporting Information); IR: $\tilde{\nu}=3274.6$ (OH), 2920.3 (CH, CH_2), 1013.2 cm^{-1} (C–O); LILBID-MS: m/z calcd for $C_{472}H_{912}N_{30}O_{320}$: 12128.3 (relating to 32 maltose units connected to the surface of third-generation PPI dendrimer **2**); found: 12100 $[M]^-$.

Maltose-modified fourth-generation PPI ***7***: The same reaction conditions and work-up procedure as that used for the synthesis of **6** were used to isolate **7** (1.26 g, 91 %) using fourth-generation PPI dendrimer **3** (0.2 g, 5.691×10^{-5} mol). ^{1}H NMR (D_2O): $\delta=1.4$–2.3 (a, d, g, j, and m), 2.3–3.35

(1′, b, c, e, f, h, i, k, l, and n), 3.35–4.55 (2–6 and 2′–6′), 4.95–5.35 ppm; ^{13}C NMR (D_2O): δ = 21–27 (a, d, g, j, and m), 51–57 (b, c, e, f, h, i, k, l, and n), 59.8 (1′), 63.4 (6), 65.2 and 65.6 (6′), 70–71.5 (2′), 72.3 (4), 74.5 and 74.55 (2 and 3′), 75.4 (5 and 5′), 75.8 (3), 84.8 and 85.3 (4′), 103.5 ppm (1); IR: $\tilde{\nu}$ = 3278.0 (OH), 2923.5 (CH, CH_2), 1014.4 cm^{-1} (C–O); LILBID-MS: *m*/*z* calcd for $C_{952}H_{1840}N_{62}O_{640}$: 24396.83 (relating to 64 maltose units connected to the surface of fourth-generation PPI dendrimer **3**); found: 24400 $[M]^-$.

Maltose-modified fifth-generation PPI ***8***: The same reaction conditions and work-up procedure as that used for the synthesis of **6** were used to isolate **8** (1.41 g, 98%) using fifth-generation PPI dendrimer **4** (0.2 g, 2.7×10^{-5} mol). ^{1}H NMR (D_2O): δ = 1.4–2.3, 2.3–3.4, 3.4–4.55, 4.95–5.35 ppm; ^{13}C NMR (D_2O): δ = 21–27, 48–57, 59.8, 63.4, 65.3 and 65.6, 70.8, 72.4, 73.5–78.0, 79.2, 83–86, 103.5 ppm (see Figure 2-SI in the Supporting Information); IR: $\tilde{\nu}$ = 3278.0 (OH), 2923.5 (CH, CH_2), 1014.4 cm^{-1} (C–O); LILBID-MS: *m*/*z* calcd for $C_{1912}H_{3824}N_{126}O_{1280}$: 49062.9 (relating to 128 maltose units connected to the surface of fifth-generation PPI-$(NH_2)_{64}$ **4**); found: 44500 $[M-14\,\text{maltose}]^-$. The detailed structural assignment is given in the Supporting Information.

Hemolysis test: Blood from healthy donors was obtained from the Central Blood Bank in Lodz. Blood was anticoagulated with 3% sodium citrate. Erythrocytes were separated from blood plasma and leukocytes by centrifugation (1000*g*, 5 min) at 4 °C and washed three times with phosphate-buffered saline (PBS) solution. Erythrocytes were used immediately after isolation. To study the effect of dendrimers on erythrocyte hemolysis, red blood cells were suspended in solutions of dendrimers (3 and 6 mg mL^{-1}) at a hematocrit of 2% and incubated 2 h at 37 °C. Next, the suspension was centrifuged (1000*g*, 5 min). For reference, red blood cells were treated with double-distilled water, which corresponds to 100% hemolysis. The percentage of hemolysis was determined on the basis of released hemoglobin in supernatants and measured spectrophotometrically from the absorbance at λ = 540 nm.

Interaction with HSA: HSA was dissolved in PBS solution (150 mmol L^{-1} NaCl, 1.9 mmol L^{-1} NaH_2PO_4, 8.1 mmol L^{-1} Na_2HPO_4, pH 7.4) at a concentration of 5 μmol L^{-1}. Fluorescence spectra were taken with a Perkin–Elmer LS-50B fluorescence spectrometer. Samples were maintained at 25 °C using a thermostat. An excitation wavelength of 295 nm was used to avoid the contribution from tyrosine residues. The emission spectra were recorded at wavelengths from 300 to 440 nm. The excitation and emission slit widths were set to 10 and 3.4 nm, respectively. Samples were kept in 1 cm-path-length quartz cuvettes and were continuously stirred. Next, the concentration of the dendrimers was increased, ranging from 0.012 to 0.600 mmol L^{-1}, by adding aliquots of dendrimer to HSA from a stock solution in PBS (3 mmol L^{-1}) and the fluorescence of the HSA tryptophan residue was measured. Before examining the fluorescence properties of the protein we checked that the dendrimers were not excited by the 295 nm wavelength and did not emit fluorescence.

Effects of dendrimers on aggregation of the prion peptide: Amyloid fibrils can be produced in vitro by exposing disease-associated peptides, such as prion peptide PrP 185-208 [KQHTVTTTTKGENFTETDVKMMER], to destabilizing conditions (adding heparin and lowering the pH). The aggregation process was monitored by using the dye thioflavin T (ThT), the fluorescence of which depends on the presence of amyloid structures. A stock solution of peptide (1.2 mmol L^{-1}) in Tris buffer pH 7.5 was diluted to a final concentration of 50 μmol L^{-1}. Then ThT and heparin were added (final concentrations of 35 μmol L^{-1} and 0.041 mg mL^{-1}, respectively) and the pH was adjusted to 5.5 with aliquots of HCl. Fluorescence measurements were performed at 37 °C (upon continuous stirring) by using a Perkin–Elmer LS-50B fluorescence spectrometer. The kinetics of aggregation was monitored by recording the fluorescence intensity. The excitation and emission wavelengths were 450 and 490 nm, respectively. The excitation and emission slit widths were set to 5 nm.

Interactions with ANS: ANS was dissolved in PBS at a concentration of 20 μmol L^{-1}. The excitation wavelength of 360 nm was used and the emission spectra were recorded from 400 to 640 nm. The excitation and emission slit widths were 10 and 3.4 nm, respectively. Then increasing aliquots of dendrimers were added from a stock solution in PBS and the wavelength of the emission maximum and the fluorescence intensity for the emission maximum were registered until there were no changes in spectral properties; this corresponded to the state of binding of all ANS molecules. To determine the binding constant (K_b) and the number of binding centers per dendrimer molecule (*n*) a double fluorometric titration technique and Scatchard–Klotz analysis[34] were employed (see the Supporting Information).

Acknowledgements

We thank the Saxonian Ministry of Science and Art, the German Research Foundation and POLPHARMA Foundation for Development of Polish Pharmacy and Medicine (grant no. 12/04/2005) for financial support.

[1] a) U. Boas, P. M. H. Heegaard, *Chem. Soc. Rev.* **2004**, *33*, 43–63; b) A. D'Emanuele, D. Attwood, *Adv. Drug Delivery Rev.* **2005**, *57*, 2147–2162; c) U. Gupta, H. B. Agashe, A. Asthana, N. K. Jain, *Biomacromolecules* **2006**, *7*, 649–658.
[2] a) U. Boas, P. M. H. Heegaard, *Recent Pat. Anti-Infect. Drug Discovery* **2006**, *1*, 333–351; b) A. R. Borges, C. L. Schengrund, *Curr. Drug Targets* **2005**, *5*, 247–254.
[3] M. W. Grinstaff, *Chem. Eur. J.* **2002**, *8*, 2839–2846.
[4] a) B. H. Zinselmeyer, S. P. Mackay, A. G. Schatzlein, I. F. Uchegbu, *Pharm. Res.* **2002**, *19*, 960–967; b) C. Dufès, I. F. Uchegbu, A. G. Schätzlein, *Adv. Drug Delivery Rev.* **2005**, *57*, 2177–2202.
[5] a) C. Douat-Casassus, T. Darbre, J.-L. Reymond, *J. Am. Chem. Soc.* **2004**, *126*, 7817–7826; b) J. Kofeod, J.-L. Reymond, *Curr. Opin. Chem. Biol.* **2005**, *9*, 656–664.
[6] D. Artemov, *J. Cell. Biochem.* **2003**, *90*, 518–524.
[7] a) S.-E. Stiriba, H. Frey, R. Haag, *Angew. Chem.* **2002**, *114*, 1385–1390; *Angew. Chem. Int. Ed.* **2002**, *41*, 1329–1334; b) R. Haag, F. Kratz, *Angew. Chem.* **2006**, *118*, 1218–1237; *Angew. Chem. Int. Ed.* **2006**, *45*, 1198–1215.
[8] a) D. A. Tomalia, A. M. Naylor, W. A. Goddard III, *Angew. Chem.* **1990**, *102*, 119–157; b) A. W. Bosman, H. M. Janssen, E. W. Meijer, *Chem. Rev.* **1999**, *99*, 1665–1688; c) G. R. Newkome, Y. He, C. N. Moorefield, *Chem. Rev.* **1999**, *99*, 1689–1746; d) Dendrimers and Other Dendritic Polymers, Wiley Series in Polymer Science (Eds.: J. M. J. Fréchet, D. A. Tomalia), Wiley, West Sussex, **2001**; e) K. Sadler, J. P. Tams, *Rev. Mol. Biotechnol.* **2002**, *90*, 195–229; f) J. M. J. Fréchet, *J. Polym. Sci., Part A: Polym. Chem.* **2003**, *41*, 3713–3725; g) L. Crespo, G. Sanclimens, M. Pons, E. Giralt, M. Royo, F. Albericio, *Chem. Rev.* **2005**, *105*, 1663–1681; h) D. Shabat, *J. Polym. Sci., Part A: Polym. Chem.* **2006**, *44*, 1569–1578; i) For recent developments, see: *New J. Chem.* **2007**, *31*, issue 7.
[9] R. Duncan, L. Izzo, *Adv. Drug Delivery Rev.* **2005**, *57*, 2215–2237.
[10] a) N. Malik, R. Wiwattanapatapee, R. Klopsch, K. Lorenz, H. Frey, J.-W. Weener, E. W. Meijer, W. Paulus, R. Duncan, *J. Controlled Release* **2000**, *65*, 133–148; b) T. Okuda, A. Sugiyama, T. Niidome, H. Aoyagi, *Biomaterials* **2004**, *25*, 537–544; c) H. Arima, Y. Chihara, M. Arizona, S. Yamashita, K. Wada, F. Hirayama, K. Uekama, *J. Controlled Release* **2006**, *116*, 64–74.
[11] H. Kobayashi, S. Kawamoto, T. Saga, N. Sato, A. Hiraga, T. Ishimori, J. Konishi, K. Togashi, M. W. Brechbiel, *Magn. Reson. Med.* **2001**, *46*, 781–788.
[12] S. Fuchs, T. Kapp, H. Otto, T. Schöneberg, P. Franke, R. Gust, A. D. Schlüter, *Chem. Eur. J.* **2004**, *10*, 1167–1192.
[13] a) R. Jevprasesphant, J. Penny, R. Jalal, D. Attwood, N. B. McKeown, A. D'Emanuele, *Int. J. Pharm.* **2003**, *252*, 263–266; b) R. Jevprasesphant, J. Penny, D. Attwood, N. B. McKeown, A. D'Emanuele, *Pharm. Res.* **2003**, *20*, 1543–1550.
[14] a) B. Klajnert, M. Bryszewska, *Bioelectrochemistry* **2002**, *55*, 33–35; b) B. Klajnert, L. Stanislawska, M. Bryszewska, B. Palecz, *Biochim. Biophys. Acta Proteins Proteomics* **2003**, *1648*, 115–126; c) D. Shcharbin, B. Klajnert, M. Bryszewska, *J. Biomater. Sci., Polym. Ed.*

2005, *16*, 1081–1093; d) M. F. Ottaviani, S. Jockush, N. J. Turro, D. A. Tomalia, A. Barbon, *Langmuir* **2004**, *20*, 10238–10254.

[15] a) N. Yahi, J. Fantini, S. Baghdiguian, K. Mabrouk, C. Tamelet, H. Rochat, J. Van Rietschoten, J. M. Sabatier, *Proc. Natl. Acad. Sci. USA* **1995**, *92*, 4867–4871; b) N. Bourne, L. R. Stanberry, E. R. Kern, G. Holan, B. Matthews, D. I. Bernstein, *Antimicrob. Agents Chemother.* **2000**, *44*, 2471–2474; c) D. I. Berstein, I. R. Stanberry, S. Sacks, N. K. Ayisi, Y. H. Gang, J. Ireland, R. J. Mumper, G. Holan, B. Matthews, T. McCharty, N. Bourne, *Antimicrob. Agents Chemother.* **2003**, *47*, 3784–3788; d) R. D. Kensinger, B. J. Catalone, F. C. Krebs, B. Wigdahl, C.-L. Schengrund, *Antimicrob. Agents Chemother.* **2004**, *48*, 1614–1623; e) H. Zhao, J. Li, F. Xi, L. Jiang, *FEBS Lett.* **2004**, *563*, 241–245; f) Y. H. Jiang, P. Emau, J. S. Cairns, L. Flanary, W. R. Morton, T. D. McCharty, D. D. Tsai, *Aids Res. Hum. Retroviruses* **2005**, *21*, 207–213.

[16] a) S. L. Cooper, C. Z. Chen, US 20026440405 (, **2002**); b) C. Z. Chen, S. L. Cooper, *Biomaterials* **2002**, *23*, 3359–3368.

[17] a) M. Stefani, C. M. Dobson, *J. Mol. Med.* **2003**, *81*, 678–699; b) R. Sabaté, M. Gallardo, J. Estelrich, *Biopolymers* **2003**, *71*, 190–195.

[18] a) S. Supattapone, H.-O. B. Nguyen, F. E. Cohen, S. B. Prusiner, M. R. Scott, *Proc. Natl. Acad. Sci. USA* **1999**, *96*, 14529–14534; b) S. Supattapone, H. Wille, L. Uyechi, J. Safar, P. Tremblay, F. C. Szoka, F. E. Cohen, S. B. Prusiner, M. R. Scott, *J. Virol.* **2001**, *75*, 3453–3461.

[19] a) P. V. Kumar, A. Asthana, T. Dutta, N. K. Jain, *J. Drug Targeting* **2006**, 14, 546–556; b) T. Dutta, N. K. Jain, *Biochim. Biophys. Acta* **2007**, *1770*, 681–686; c) M.-A. Zanta, O. Boussif, A. Adib, J.-P. Behr, *Bioconjugate Chem.* **1997**, *8*, 839–844; d) S. S. Diebold, M. Kursa, E. Wagner, M. Cotten, M. Zenke, *J. Biol. Chem.* **1999**, *274*, 19087–19094; e) K. Kunath, A. von Harpe, D. Fischer, T. Kissel, *J. Controlled Release* **2003**, *88*, 159–172.

[20] a) M. Liu, J. M. J. Fréchet, *J. Controlled Release* **2000**, *65*, 121–131; b) C. Kojima, K. Kono, K. Maruyama, T. Takagishi, *Bioconjugate Chem.* **2000**, *11*, 910–917; c) G. Pan, Y. Lemmouchi, E. O. Akala, O. Bakare, *J. Bioact. Compat. Polym.* **2005**, *20*, 113–128.

[21] a) D. M. Ratner, E. W. Adams, M. D. Disney, P. H. Seeberger, *ChemBioChem* **2004**, *5*, 1375–1383; b) W. Morelle, J.-C. Michalski, *Current Pharmaceutical Design* **2005**, *11*, 2615–2645.

[22] N. Sharon, *Biochim. Biophys. Acta Gen. Subj.* **2006**, *1760*, 527–537.

[23] Reviews: a) K. Bezouška, *Mol. Biotechnol.* **2002**, *90*, 269–290; b) R. Roy, *Trends Glycosci. Glycotechnol.* **2003**, *15*, 291–310; c) K. J. Doores, D. P. Gamblien, B. G. Davis, *Chem. Eur. J.* **2006**, *12*, 656–665.

[24] a) K. Aoi, K. Itoh, M. Okada, *Macromolecules* **1995**, *28*, 5391–5393; b) J. P. Thompson, C.-L. Schengrund, *Biochem. Pharmacol.* **1998**, *56*, 591–597; c) M.-K. Baek, R. Roy, *Bioorg. Med. Chem.* **2002**, *10*, 11–17; d) A. C. Choudhury, M. Kitaoka, *Eur. J. Org. Chem.* **2003**, 2462–2470; e) E. K. Woller, E. D. Walter, J. R. Morgan, D. J. Singel, M. J. Cloninger, *J. Am. Chem. Soc.* **2003**, *125*, 8820–8826; f) M. Köhn, J. Benito, C. O. Mellet, T. K. Linhorst, J. M. García Fernández, *ChemBioChem* **2004**, *5*, 771–777; g) K. H. Schlick, R. A. Udelhoven, G. C. Strohmeyer, M. J. Cloninger, *Mol. Pharmaceutics* **2005**, *2*, 295–301; h) T. Dam, S. Oscarson, R. Roy, S. K. Das, D. Page, F. Macaluso, C. F. Brewer, *J. Biol. Chem.* **2005**, *280*, 8640–8646; i) M. L. Wolfenden, M. J. Cloninger, *Bioconjugate Chem.* **2006**, *17*, 958–966; j) G. Thoma, A. G. Streiff, A. G. Katapodis, R. O. Duthaler, N. H. Voelcker, C. Ehrhardt, C. Masson, *Chem. Eur. J.* **2006**, *12*, 99–117; k) K. Marotte, C. Preville, C. Sabin, M. Moume-Pymbock, A. Imberty, R. Roy, *Org. Biomol. Chem.* **2007**, *5*, 2953–2961.

[25] a) H. Baigude, K. Katsuraya, K. Okuyama, Y. Yachi, S. Sato, T. Uryu, *J. Polym. Sci., Part A: Polym. Chem.* **2002**, *40*, 3622–3633; b) H. Baigude, K. Katsuraya, K. Okuyama, S. Tokunaga, T. Uryu, *Macromolecules* **2003**, *36*, 7100–7106; c) D. Appelhans, Y. Zhong, H. Komber, P. Friedel, U. Oertel, U. Scheler, N. Morgner, D. Kuckling, S. Richter, B. Brutschy, B. Voit, *Macromol. Biosci.* **2007**, *7*, 373–383.

[26] a) H. Baigude, K. Katsuraya, K. Okuyama, K. Hatanaka, E. Ikeda, N. S. Shibata, T. Uryu, *J. Polym. Sci., Part A: Polym. Chem.* **2004**, *42*, 1400–1414; b) H. Baigude, K. Katsuraya, S. Tokunaga, N. Fujiwara, M. Satoyama, T. Magome, K. Okuyama, G. Borjihan, T. Uryu, *J. Polym. Sci., Part A: Polym. Chem.* **2005**, *43*, 2195–2206.

[27] O. Stern, M. Volmer, *Physik. Zeitschr.* **1919**, *20*, 183–188.

[28] D. Bhadra, A. K. Yadav, S. Bandra, N. K. Jain, *Int. J. Pharm.* **2005**, *295*, 221–223.

[29] a) B. Klajnert, M. Cortijo, M. Bryszewska, J. Cladera, *Biochem. Biophys. Res. Commun.* **2006**, *339*, 577–582; b) B. Klajnert, M. Cortijo-Arellano, J. Cladera, M. Bryszewska, *Biochem. Biophys. Res. Commun.* **2006**, *345*, 21–28.

[30] B. Klajnert, J. Cladera, M. Bryszewska, *Biomacromolecules* **2006**, *7*, 2186–2191.

[31] D. Shcharbin, B. Klajnert, V. Mazhul, M. Bryszewska, *J. Fluoresc.* **2003**, *13*, 519–524.

[32] K. Tsutsumiuchi, K. Aoi, M. Okada, *Polym. J.* **1999**, *31*, 935–941.

[33] N. Morgner, H.-D. Barth, B. Brutschy, *Aust. J. Chem.* **2006**, *59*, 109–114.

[34] G. Scatchard, *Ann. N. Y. Acad. Sci.* **1949**, *51*, 660–672.

Received: February 24, 2008
Published online: June 24, 2008

